Green Synthesis of Silver Nanoparticles Derived from *Phyllanthus amarus* Leaf Extract for Environmental and Biological Applications

Ghaferah H. Al-Hazmi,[a] Oyebola Elizabeth Ogunbamowo,[b,c] Lamia A. Albedair,[a] Abidemi Mercy Babatimehin,[b,d] Edwin Andrew Ofudje ,[b] Moamen S. Refat,[e] Kholoud K. Alzahrani,[f] and Ali El-Rayyes [g]

This study reports silver nanoparticles (AgNPs) synthesis through a green, facile, and eco-friendly route using aqueous leaf extract of *Phyllanthus amarus* as both reducing and stabilizing agent. GCMS screening of the plant extract affirmed the presence of phytochemicals such as flavonoids, polyphenols, and other biomolecules responsible for the reduction and stabilization of synthesized nanoparticles. The biosynthesis was confirmed with a visible color change from pale yellow to brown with UV–Visible spectroscopy indicated AgNPs formation within 400 to 450 nm. X-ray diffraction (XRD) revealed three distinct peaks corresponding to (111), (200), and (220) crystal planes, while transmission electron microscopy (TEM) indicated circular-shaped particles with particle size in the range of 10.02 to 28.5 nm. The optical activity of the synthesized nanoparticles was confirmed by its ability to sense the presence of selected metals such as manganese, iron, lead, arsenic, and cadmium ions, demonstrating potential environmental applications. In addition, the as-prepared AgNPs exhibited antimicrobial effects against gram-positive and gram-negative bacteria. The green synthesis method using *P. amarus* offers a low-cost and sustainable route to stable AgNPs with bi-functional properties suitable for biological and environmental applications.

DOI: 10.15376/biores.21.2.3518-3542

Keywords: Antimicrobial; Green synthesis; Optical activity; Nanoparticles; Phytochemicals

Contact information: a: Department of Chemistry, College of Science, Princess Nourah bint Abdulrahman University, P.O. Box 84428, Riyadh 11671, Saudi Arabia; b: Department of Chemical Sciences, Mountain Top University, Ibafo, Ogun State, Nigeria; c: Department of Medical Biochemistry, Lagos State University College of Medicine, Ikeja, Lagos, Nigeria; d: Department of Biochemistry, Lagos State University, Ojo, Lagos, Nigeria; e: Department of Chemistry, College of Science, Taif University, P.O. Box, 11099, Taif 21944, Saudi Arabia; f: Department of Biology, University College of Umluj, University of Tabuk, Umluj, Tabuk, Saudi Arabia; g: Center for Scientific Research and Entrepreneurship, Northern Border University, 73213, Arar, Saudi Arabia; ** Corresponding author: oyebolaogunbamowo818@gmail.com*

INTRODUCTION

The escalating global health challenge posed by multidrug-resistant (MDR) bacterial pathogens has amplified the urgency for novel antimicrobial strategies, as conventional antibiotics gradually lose efficacy and contribute to treatment failures and increased mortality. Heavy metal pollution, on the other hand is becoming an urgent worldwide problem that has a big influence on both health and the economy. For instance, the World Health Organization lists mercury (Hg) as one of the top 10

substances of important public health concern, and lead (Pb) as one of the most common dangerous heavy metals in the environment and water (WHO 2013). Heavy metals (HMs) are elements with an atomic number greater than 20 and a density exceeding 5 g/cm³, such as Pb, Cd, As, Cu, Co, Fe, Zn, Hg, Cr, and Ag (Babatimehin *et al*. 2025a). Because of their water solubility and environmental mobility, they can readily contaminate soil, water, and air *via* agricultural and industrial activities, resulting in their uptake by aquatic organisms, plants, animals, and humans (Lokhande *et al*. 2011; Akinhanmi *et al*. 2020, Ofudje *et al.* 2021). Their persistence and tendency to bioaccumulate pose huge risks to ecological and human health, causing hepatic, renal, neurological, cardiovascular, and skeletal damage primarily through mechanisms including enzymatic inhibition and oxidative stress (Paithankar *et al*. 2021; Jomova *et al*. 2025). With their widespread presence in the environment coupled with their cumulative toxicity, detecting their presence is vital for effective management.

Heavy metals detection can be achieved *via* analytical methods such as Inductively Coupled Plasma–Mass Spectrometry (ICP–MS), Atomic Absorption Spectroscopy (AAS), and X-Ray Fluorescence (XRF), with each offering different levels of accuracy, sensitivity, and cost-effectiveness (Helim *et al*. 2024; Nadumane *et al*. 2024). Nevertheless, these techniques face setbacks such as interference from other substances, complex sample preparation, high operational costs, and limited accessibility, suggesting the need for more rapid, affordable, and standardized detection methods (Abdelmonem *et al*. 2025; Kyabutwa *et al*. 2025).

Nano-science has gained great interest as a promising alternative, utilizing materials designed at the nanometer scale, where distinctive size-dependent characteristics enhance their performance and reactivity (Chen *et al*. 2019; Ogunbamowo *et al.* 2025). These nanomaterials possess optical properties that are adjustable with large surface areas and optical potency making them suitable for applications in sensing environmental contaminants (Babatimehin *et al*. 2025b). Nanoparticles fabrication *via* green approach with the use of plant extracts offers an environmentally friendly approach, which utilized phytochemicals as organic reducing and stabilizing agents which eventually eliminate the use of hazardous chemicals (Fahimmunisha *et al*. 2020).

Silver nanoparticles (AgNPs) have emerged as a promising alternative because of their broad-spectrum antimicrobial activities, coupled with their optical potential, which make them attractive platforms in biomedical and environmental applications (Bruna *et al.* 2021). Traditional physical and chemical methods for synthesizing AgNPs often rely on harsh reducing agents, high energy consumption, and by-product generation, raising environmental and biocompatibility concerns (Duman *et al*. 2024). In contrast, green synthesis approaches—particularly those mediated by plant extracts, offer eco-friendly, low-cost, and scalable routes (Babatimehin *et al*. 2025b). Plant phytochemicals such as flavonoids, polyphenols, terpenoids, alkaloids, and proteins can function as reducing and capping agents, enabling one-step nanoparticle formation under mild conditions while conferring stability and biocompatibility to the nanomaterial (Dhir *et al*. 2024). Compared to conventional methods, plant-mediated synthesis minimizes toxic residues and aligns with the principles of sustainable and green chemistry (Babatimehin *et al*. 2025b).

Within the realm of phytogenic nanoparticle synthesis, *Phyllanthus amarus* (family *Euphorbiaceae*) is a medicinal plant recognized for its rich pharmacological properties, including hepatoprotective, antioxidant, antiviral, and anti-inflammatory effects (Ajitha *et al*. 2018; Joseph *et al*. 2021). Its leaves are known to contain bioactive

compounds including tannins, polyphenols, alkaloids, and flavonoids, which are capable of reducing metal ions (M^+) to elemental metals (M^0) while acting as stabilizing agents (Ajitha *et al*. 2018; Joseph *et al*. 2021). Previous reports have documented the feasibility of *Phyllanthus amarus* in nanoparticle synthesis, with evidence of antimicrobial and antioxidant activities in the resulting AgNPs (Ajitha *et al*. 2018; Habeeb *et al*. 2022).

Despite these promising findings, existing studies frequently lack deep correlation between phytochemical constituents, nanoparticle morphology, and functional performance, and often they do not evaluate catalytic or environmental sensing applications. Moreover, comprehensive physicochemical characterization and mechanistic insight into the antimicrobial and catalytic behavior of *P. amarus*-derived AgNPs remain limited in the literature. To address these gaps, the present study aimed to synthesize AgNPs using *P. amarus* leaf extract (L-AgNPs), and to thoroughly investigate their structural, morphological, and chemical properties using spectroscopic and microscopic techniques. In addition, the antimicrobial performance of these biogenic AgNPs were evaluated against selected Gram-positive and Gram-negative bacterial strains. In addition, the sensing ability of the AgNPs against selected metals was explored. By elucidating the links between synthesis parameters, nanoparticle features, and functional efficacy, this study aspired to contribute to the advancement of green nanotechnology with dual biomedical and environmental relevance.

EXPERIMENTAL

Collection of Sample, Extract Preparation, and Phytochemical Analysis

Phyllanthus amarus plant was collected from a farm at Alagbado area in Ifo local government area of Ogun State, Nigeria. The plant was identified by specialists at the Botany department, Lagos State University, Ojo, Lagos and given the voucher number LSH-001287. Thereafter it was deposited in the Herbarium of the same University. The leaf sample collected was washed several times with distilled water. About 10 g of the clean leaf sample was weighed, put in a beaker and mixed with 100 mL of distilled water, and boiled for 15 min. The mixture was allowed to cool and filtered with Whatman filter paper No. 1, and the extract was kept for future use in a bottle and kept inside a refrigerator at 4 °C. The plant extract was subjected to GC-MS analysis (Agilent Technologies 7820A Gas Chromatograph, USA) for the determination of the phytonutrients present in the plant.

Bio-synthesis of Silver Nanoparticles

Silver nitrate solutions of 1 and 3 mM were accurately prepared by dissolving 0.170 and 0.51 g of silver nitrate (Sigma Aldrich, India) salt respectively for obtaining two different concentrations. The salt samples were taken in a well-labeled standard flask and filled up to the one-liter mark with deionized water. These were stored in amber bottles in the dark to prevent auto-oxidation reaction of silver with light. To 10 mL of the leaf extract was added 90 mL of 1 mM $AgNO_3$ solution, and the mixture was mixed well by shaking in an orbital shaker and left for 30 min.

The change in the color of the mixture confirmed the nanoparticles formation, which was monitored using UV-Vis Spectrophotometer (Model SM 7504, Shanghai, China). The synthesized L-AgNPs formed was optimized by varying the extract concentration, pH, and temperature.

Characterization of L-AgNPs

The L-AgNPs synthesized was characterized using UV-Visible spectrophotometer (Model SM 7504, Shanghai, China), while X-ray diffraction (XRD) measurement was done on Rigaku Miniflex 600, diffractometer (Japan) for crystallographic examination and peaks were compared with those found in the JCPDS. Fourier transform infra-red spectroscopy (Thermo Fisher Scientific Cary 630 instrument, USA) was used for the identification of the functional groups. Spectra were acquired using the KBr pellet approach, in which sample to KBr ratio of 1% to 99% KBr (w/w) was used, homogenized, and thereafter compressed into pellet. The EDAX showed the elemental composition of the synthesized L-AgNPs using a Shimadzu EDX-7200. The chemical constituent of the sample was achieved using energy-dispersive X-ray spectroscopy (EDX) coupled with scanning electron microscope (SEM, Hitachi S-3000H Japan). For TEM investigation, the prepared nanoparticles were dispersed in distilled water and then sonicated for 15 min to form a uniform suspension. A small drop of the suspension was thereafter deposited onto a copper grid and left to dry before imaging with a TEM (Tecnai 20 G2 FEI, Netherlands).

Application of Synthesized AgNPs to Metal Ions Sensing

The colorimetric sensor potency of the fabricated nanoparticles (AgNPs) was employed to detect metal ions. In a typical assay, 1.0 mL of the prepared nanoparticles was reacted with 1 mL of a 100 μM solution the metal ion. The mixtures were incubated at 35 °C. Sensing was done by observing two main parameters which are visible color changes in the solution as well as variations in absorption intensity, as measured by UV–Vis spectroscopy. Each measurement was done thrice, and the reported values represent the average mean.

Application of Synthesized AgNPs to Antibacterial Study

The antibacterial activity of the fabricated AgNPs was examined against *Staphylococcus aureus* (*S. aureus*) and *Escherichia coli* (*E. coli*) using the well diffusion method as reported by Dawadi *et al*. (2021). Mueller–Hinton agar plates were made and inoculated with 0.2 mL of a standardized bacterial suspension, which was later spread across the agar surface with a sterile Pasteur pipette and a hockey stick–shaped glass spreader. Two wells, each 6 mm in diameter, were then made into the agar using a flame-sterilized cork borer. The plates were left to stand for 5 min before the test samples were introduced to the wells and kept at room temperature for 30 min.

Analysis of Minimum Inhibitory Concentrations (MIC) and Minimum Bactericidal Concentrations (MBC)

The minimum inhibitory concentration (MIC), which indicates the lowest concentration of the nanoparticles that completely inhibited visible microbial growth was examined using the broth dilution method (Dawadi *et al*. 2021). A stock solution of the as-prepared nanoparticles was made from the mixture of 4 mL of peptone water and 2 mL of the nanoparticle suspension. Each flask was inoculated with three drops of a standardized broth culture of the test organisms (*S. aureus* or *E. coli*) and thereafter, incubated at 37 °C for 24 h. After the incubation period, the MIC value was evaluated as the lowest concentration of nanoparticles that exhibited no visible turbidity, signifying complete inhibition of microbial growth. To evaluate the MBC value, a sub-culturing procedure was carried out following the MIC assay. Samples from tubes indicating no

visible growth were aseptically streaked onto sterile nutrient agar plates, which were then incubated at 37 °C for 24 h. The MBC was identified as the lowest concentration of the nanoparticles that resulted in no bacterial colony formation on the agar surface, confirming a bactericidal effect and suggesting that the nanoparticles had killed the microorganisms rather than merely inhibiting their growth.

RESULTS AND DISCUSSION

Characterization of *P. amarus* Extract

The extract was subjected to GC-MS analysis to determine the phyto-nutrients present in the plant extract which may be the main purpose of stabilization and capping agent for the synthesis. It was observed from the GC-MS that the qualitative bio-molecular constituents of the plants contained different compounds from phenols, terpenoids, fatty acids, organic acids, flavonoids, and fatty acids alkaloids, among others (Njideaka *et al*. 2024). The GC-MS chromatogram is as shown in Fig. 1. Table 1 shows the retention time, peak area (%), and structures confirming the presence of 2-H-coumaranone (14.55%), 4H-pyran-4-one (8.04%), benzoic acid (7.38%), hydroxymethylfurfural (4.25%), uracil (5.53%), n-hexadecanoic acid (3.84%), 9-octadecenoic acid (2.74%), patchouli alcohol (3.38%), eugenol (1.83%), and γ-tocopherol (2.30%). Their presence is likely to have contributed greatly to the reduction and stabilization processes leading to the nanoparticle formation (Moideen and Prabha 2022: Md Monir *et al.* 2024).

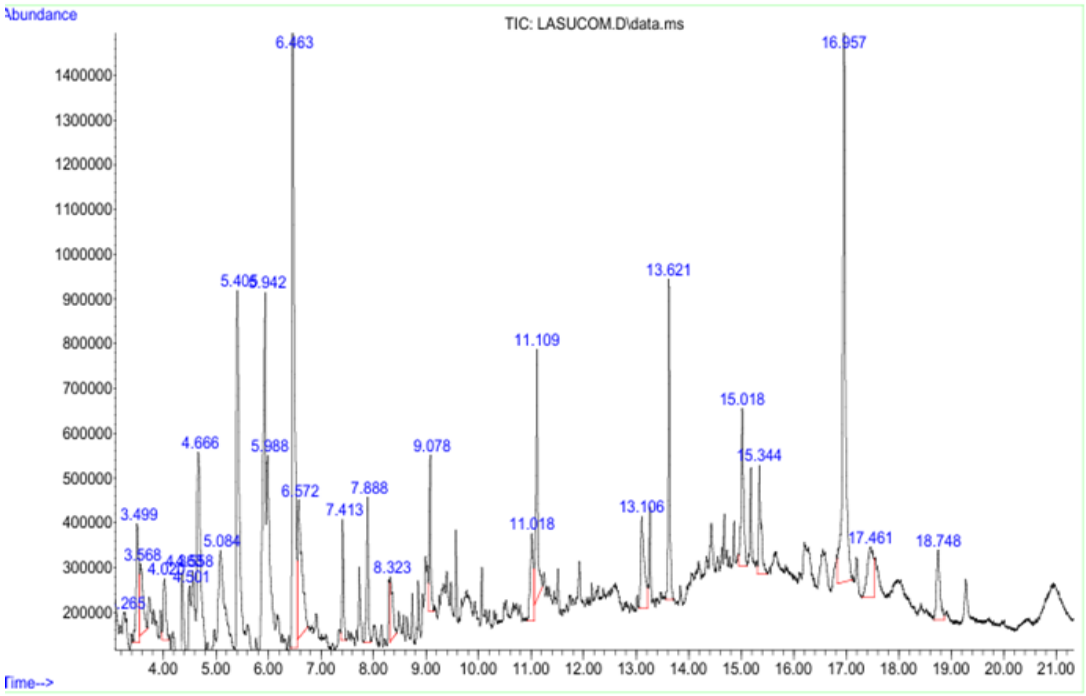

Fig. 1. GC-MS chromatogram of *P. amarus* plant

The reduction of Ag^{+} to Ag^{0} is primarily facilitated by phytochemicals such as 2-H-coumaranone, hydroxymethyl-furfural, 4H-pyran-4-one, and eugenol containing carbonyl, hydroxyl, and aldehyde groups. These compounds are known to possess strong

electron-donating properties that promote the reduction of Ag^{+} ions (Md Monir *et al*. 2024). After reduction process, the presence of fatty acids such as 9-octadecenoic acid (oleic acid) and n-hexadecanoic acid (palmitic acid), terpenoids such as antioxidants, and patchouli alcohol such as γ-tocopherol as well as benzoic and uracil acid in the extract can enhance the stability and capping of the synthesized AgNPs.

Table 1. GC-MS Analysis of the *Phyllanthus amarus* Plant

RT (min)	Area (%)	Compound	Structure
3.265	1.19	2-Cyclopenten-1-one	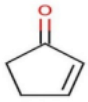
3.499	2.65	2-Butenedioic acid	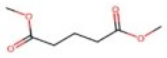
3.568	1.63	Propionic acid	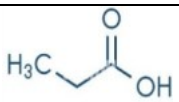
4.020	1.22	Benzene-acetaldehyde	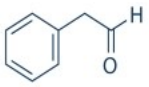
4.363	1.86	Furan	
4.501	1.19	2,5-Furandicarboxaldehyde	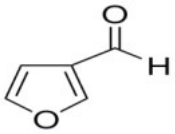
4.558	1.96	6-Methyl-2-pyrazinylmethanol	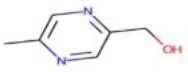
4.666	5.53	Uracil	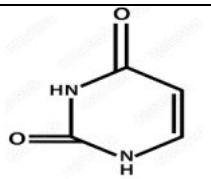
5.405	8.04	4H-Pyran-4-one	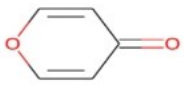

RT (min)	Area (%)	Compound	Structure
5.942	7.38	Benzoic acid	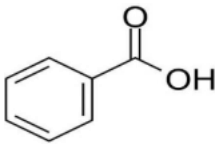
6.463	14.55	2-H-Coumaranone	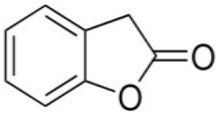
6.572	4.25	Hydroxymethylfurfural	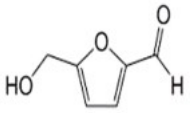
7.413	1.44	2-Methoxy-4-vinylphenol	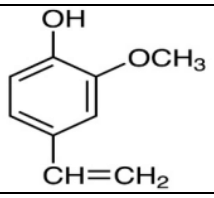
7.888	1.83	Eugenol	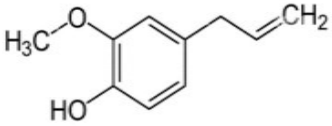
8.323	1.41	DL-Proline	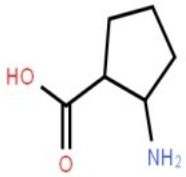
9.078	1.70	3-Octadecene	
11.018	2.22	Benzene-acetic acid	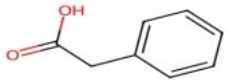
11.109	3.38	Patchouli alcohol	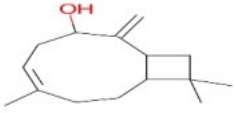
13.106	2.56	n- Decanoic acid	

RT (min)	Area (%)	Compound	Structure
13.621	3.84	n-Hexadecanoic acid	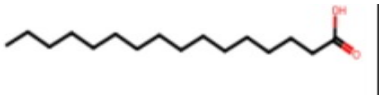
15.018	2.74	9-Octadecenoic acid	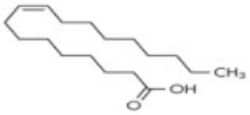
16.957	11.64		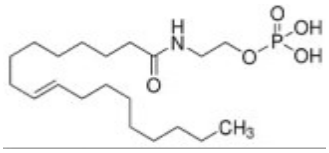
17.461	2.30	gamma-Tocopherol	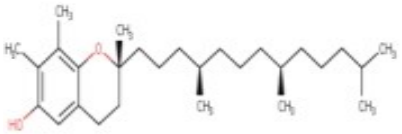

Formation of AgNPs and Optimization Studies

The formation of the synthesized L-AgNPs was monitored for change in color and the SPR value with UV-Visible spectrophotometer. The optical characteristics of the formation were seen from color change of pale yellow to deep brown after 30 min of addition of silver nitrate solution (Fig. 2). The UV-Visible spectrophotometer changed from an initial 400 nm to 450 nm, confirming the formation of L-AgNPs. Figure 3 depicts the UV–Visible absorption spectra of L-AgNPs synthesized with 1 mM $AgNO_3$ after different incubation times up to 48 h. All spectra demonstrated a prominent absorbance band between 400 and 450 nm, which can be attributed to the characteristic surface plasmon resonance (SPR) of AgNPs, indicating their formation (Khalir *et al*. 2020). At the beginning, the extract gave a broad and less intense spectrum. However, with increase in the incubation time from 1.0 h to 48 h, the absorbance intensity rose progressively, and the peak becomes sharper. This is an indication of the reduction of Ag^+ ions to Ag^0 nanoparticles as well as the subsequent growth and stabilization of the nanoparticles formed over time (Khorrami *et al*. 2019). At 48 h, maximum absorbance was reached, suggesting the complete synthesis of the nanoparticles. Slight variations in particle size or degree of aggregation were reflected by the minor shifts in the peak position across the spectra. Figure 4 depicts the UV–Visible absorption spectra of L-AgNPs synthesized with 3 mM $AgNO_3$ at different incubation times up to 48 h. Just as the prepared AgNPs with 1 nM of $AgNO_3$, all the spectra gave a prominent absorption band in the range of 400 and 450 nm, which is a prominent property of the SPR of AgNPs (Anandalakshmi *et al.* 2016). In comparison with the extract, which gave a broad and lower-intensity curve, the spectra measured after 1.0 h to 48 h indicated a gradual increase in absorbance intensity and a more defined peak. With a rise in the incubation period, the absorbance intensity increases sharply, attaining a maximum absorption band after 48 h, indicating that the reaction attains completion at this stage.

Fig. 2. (a) Leaf extract of *Phyllanthus amarus*; (b) L-AgNPs synthesised with 1 mM $AgNO_3$ after 30 min, and (c) L-AgNPs synthesised with 3 mM $AgNO_3$ after10 min of incubation

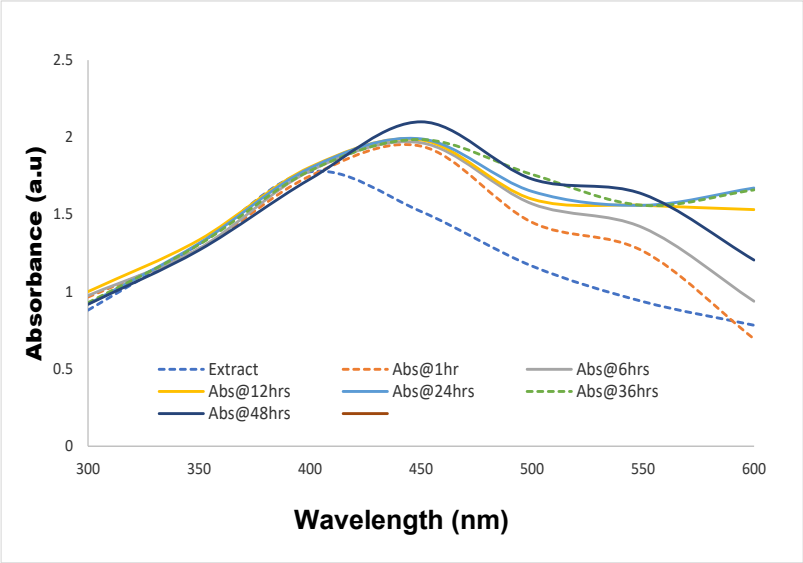

Fig. 3. UV–Visible spectra of synthesized L-AgNPs with 1 mM $AgNO_3$ after 48 h of incubation

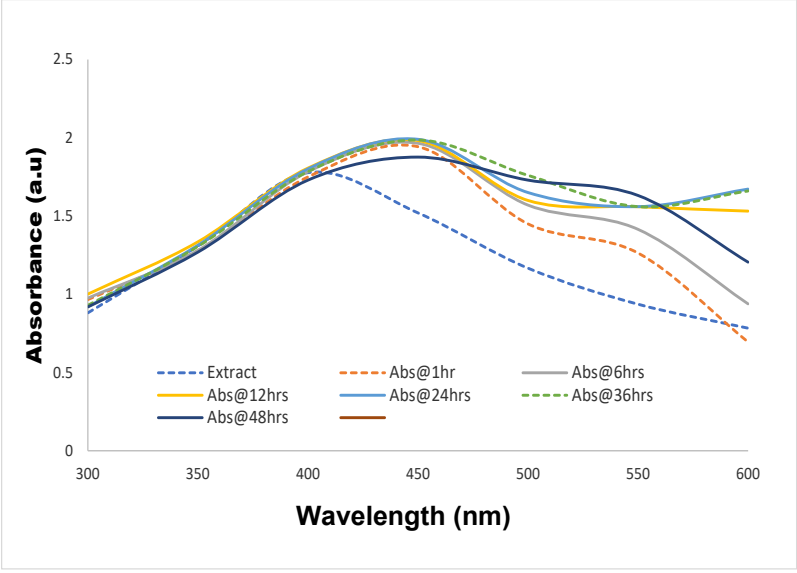

Fig. 4. UV–Visible spectra of synthesized L-AgNPs with 3 mM $AgNO_3$ after 48 h of incubation

The UV–Visible spectra of L-AgNPs prepared at different precursor concentrations (1 and 3 mM $AgNO_3$) under various pH conditions (Figs. 5 and 6) demonstrated the combined effects of both parameters' pH on the formation, stability, and optical behavior of the nanoparticles. In both spectra, the successful synthesis of AgNPs was confirmed with the appearance of a distinct SPR band in the range of 400 to 450 nm (Ogunbamowo *et al*. 2025; Babatimehin *et al*. 2025a). The sharpness, intensity, and position of the SPR peaks varied notably across pH levels, indicating differences in degree of aggregation, particle size distribution, and nanoparticle yield. As the pH rose to 10, the absorbance intensity was reduced, and a slight red-shift in the SPR peak was observed, indicating the aggregation of nanoparticles or the growth of larger particles as a result of the excessive availability of hydroxide ions (Nkosi *et al*. 2024). On the other hand, at neutral pH (pH 7), the relatively weaker absorbance suggests incomplete nanoparticle formation caused by slower reduction rates.

Thus, the most favorable conditions for synthesis of stable, well-dispersed L-AgNPs for the 1 mM solution was observed in the range of pH 8 to 9. The nanoparticles formed using 3 mM $AgNO_3$ remained relatively stable even at pH 10, unlike in the 1 mM condition, indicating that the higher concentration of silver ion improved the kinetics of the reduction and stabilized the nanoparticles against aggregation in alkaline environs. The work done by Velgosova *et al*. (2025) with the use of *Rosmarinus officinalis* for the synthesis of AgNPs found that when pH values were ≤ 5.5, it gave lower intensity and broader SPR bands, but that at a higher of pH 8 and pH 10, a well-defined and symmetric peaks were seen, indicating uniform, and stable nanoparticles. Ibrahim *et al.* (2024) which explored green synthesis *via Vachellia tortilis* leaf extract, also reported that basic conditions of pH 10 favors the synthesis rate for the formation of AgNPs at 70 °C.

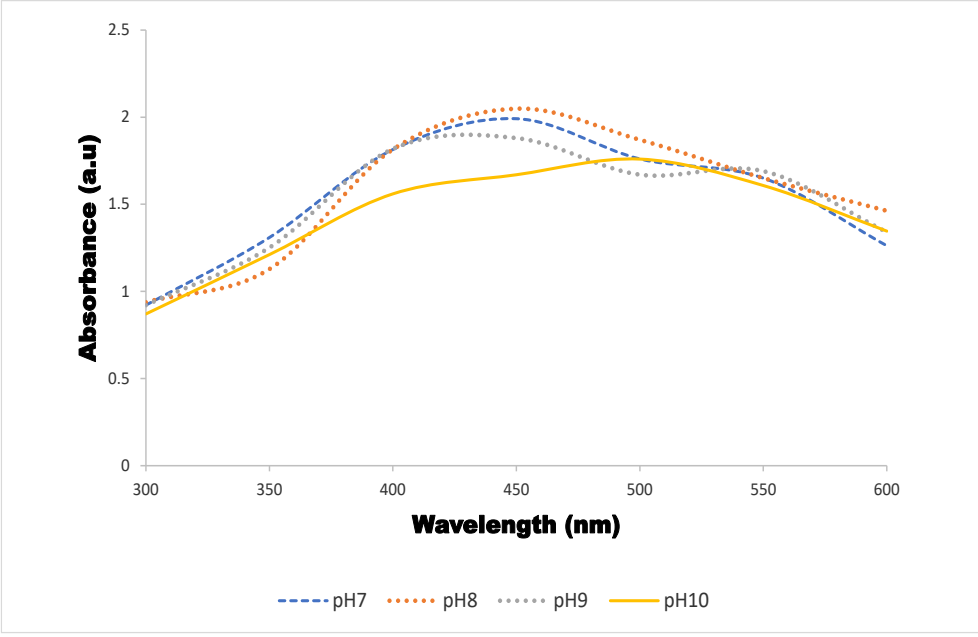

Fig. 5. UV-Visible spectra of pH gradient of L-AgNPs synthesized from 1 mM $AgNO_3$

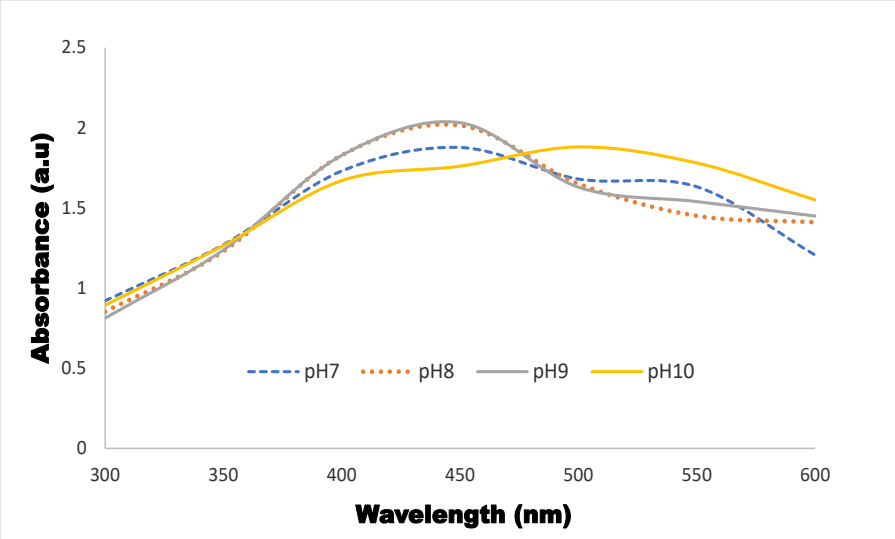

Fig. 6. UV-Visible spectra of pH gradient of L-AgNPs synthesized from 3 mM $AgNO_3$

The UV–Visible plots in Figs. 7 and 8 indicate the effect of reaction temperature (40 to 80 °C) on the synthesis of L-AgNPs. Across all tested temperatures, there were visible distinct SPR bands between 400 and 450 nm, confirming the successful synthesis of silver nanoparticles (Anandalakshmi *et al.* 2016; Ahmed *et al*. 2024). But it was observed that the shape and intensity of the SPR peaks varied slightly with temperature, indicating that temperature affected the rate of reduction of silver ion, stability, and particle nucleation of the nanoparticle.

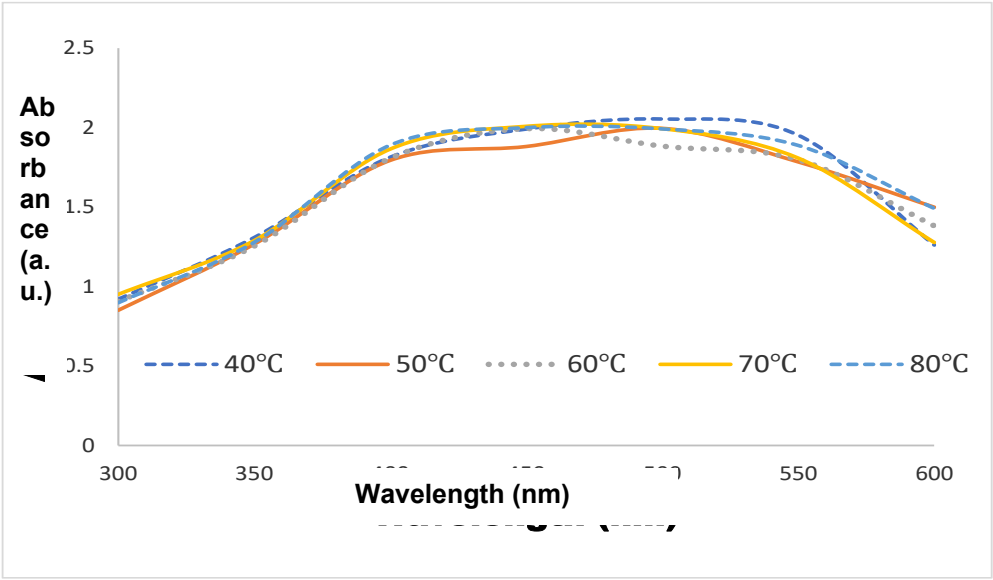

Fig. 7. UV-Visible spectra of L-AgNPs synthesised with 1 mM $AgNO_3$ at different temperatures.

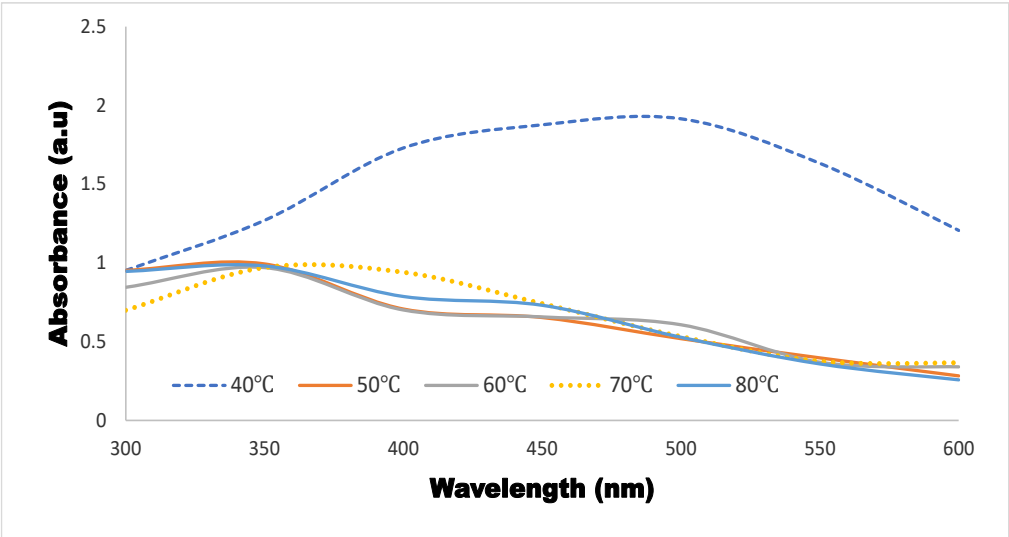

Fig. 8. UV-Visible spectra of L-AgNPs synthesised with 3 mM $AgNO_3$ at different temperatures.

The spectra at lower temperatures (40 to 50 °C) exhibited moderately intense SPR bands, suggesting that the rate of nanoparticle formation was relatively slow, giving rise to broader peaks, and wider particle size distribution (Maimaiti *et al.* 2024; Nkosi *et al*. 2024). However, the absorbance intensity increased at intermediate temperatures (60 to 70 °C, with the SPR bands becoming more defined and sharper. The sharpness of the SPR peak within this temperature range suggests that most of the silver ions were efficiently reduced, and the nanoparticles exhibited high colloidal stability (Ahmed *et al*. 2024; Maimaiti *et al*. 2024; Nkosi *et al*. 2024). This behavior remains strong even at higher temperature (80 °C), though the peak shows a slight broadening and possible red-shift which might be an indicative of the formation of slightly larger nanoparticles or aggregation because of rapid reduction and uncontrolled nucleation at higher temperatures (Ahmed *et al*. 2024; Maimaiti *et al*. 2024).

Characterization of the AgNPs

The X-ray diffraction (Fig. 9) patterns of the raw leaf and leaf-mediated silver nanoparticles (L–AgNPs) synthesized at 1 and 3 mM $AgNO_3$ concentrations reveal clear structural differences among the samples. The raw leaf diffractogram exhibited a broad pattern without any sharp peaks, suggesting that the structure was dominated by amorphous nature. Such behavior is typical of plant-based materials composed mainly of cellulose, hemicellulose, lignin, and other organic constituents. On the other hand, the diffractogram of the L–AgNPs synthesized demonstrated sharp peaks at 2θ values around 38.1°, 44.1°, and 64.3°, assigned to the planes of (111), (200), and (220) which are a characteristic of face-centered cubic metallic silver (Albadawi *et al.* 2024: Zeheri *et al.* 2025). The presence of these peaks affirms the formation of crystalline AgNPs *via* successful reduction of silver ions (Ag^+) to metallic silver (Ag^0).

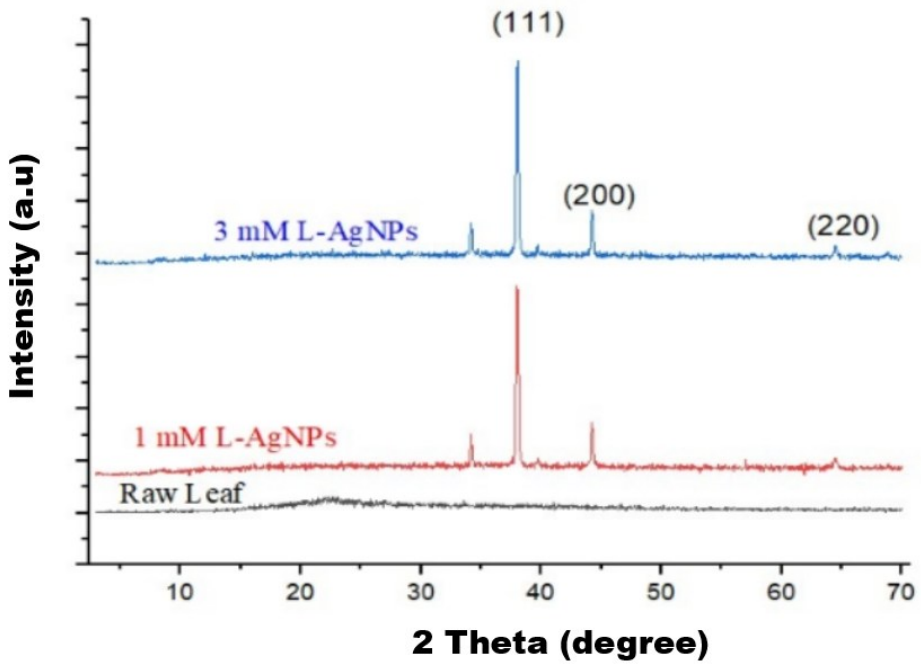

Fig. 9. XRD plot of L-AgNPs synthesized compared to raw leaf

The FTIR spectra revealed the raw leaf and the synthesized L–AgNPs showed the various functional groups responsible for silver reduction and stabilization of nanoparticles formation, as presented in Fig. 10. The presence of O–H stretching vibrations of hydroxyl groups in alcohols, phenolics, and polysaccharides were seen in the spectrum of the raw leaf at 3468 cm^{-1} (Akalin 2024; Khan *et al*. 2025). Peaks correspond to C–H stretching of aliphatic groups were observed near 2922 to 2850 cm^{-1}, while those due to the C=O stretching of amide I or conjugated carbonyl groups in proteins and flavonoids were observed around 1631 to 1705 cm^{-1}. In addition, peaks associated with C–N and C–O stretching vibrations of amines and alcohols were noticed at 1381 to 1423 cm^{-1} and 1052 to 1105 cm^{-1}, respectively (Fahim *et al.* 2024; Babatimehin *et al*. 2025a). These functional groups can act as natural reducing and capping agents for the formation of nanoparticle synthesis (Akalin 2024; Khan *et al*. 2025). In the L–AgNPs FTIR spectrum, majority of the initial peaks were still present though they showed noticeable shifts in position and reduced intensity, suggesting their involvement in the reduction of Ag^{+} ions to metallic Ag^{0}. The O–H band was seen at 3455 cm^{-1} and it became broader and less intense, while the shift and decrease in intensity of the carbonyl band from 1631 to 1705 cm^{-1} to 1630 cm^{-1} confirm the involvement of carbonyl groups in nanoparticle formation (Palanisamy *et al*. 2024). Khan *et al*. (2025) and Abbas *et al*. (2024) reported similar spectral changes in the green synthesis of AgNPs using *Momordica charantia* and *Withania coagulans* leaves, corroborating the bioreduction and stabilization role of phytochemicals.

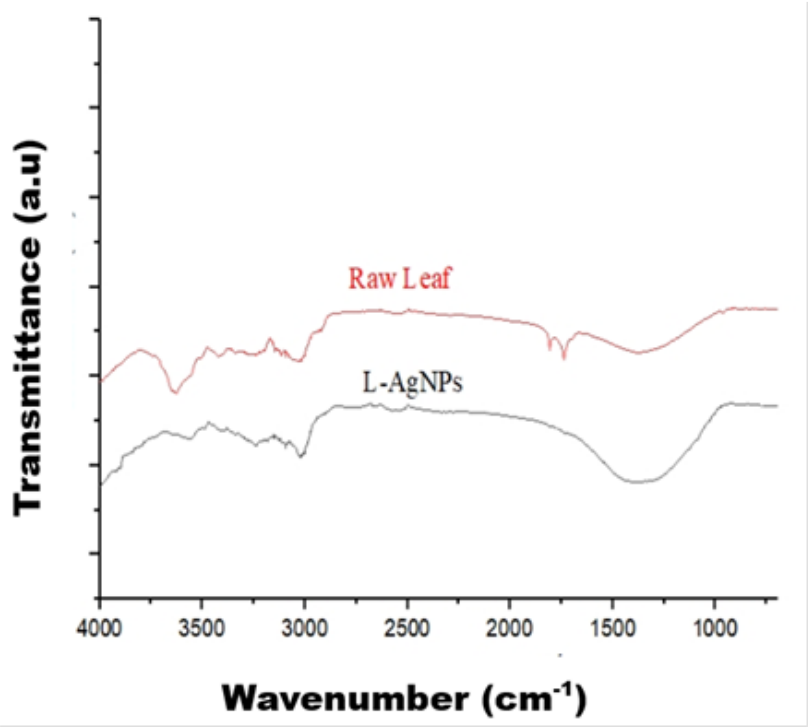

Fig. 10. FT-IR spectra of L-AgNPs synthesized at 3 mM $AgNO_3$ compared to raw leaf

The chemical composition of the prepared leaf-mediated AgNPs as is presented in Table 2 confirms the presence of silver (Ag) as the dominant metallic component, with corresponding weight concentration of 42.1% and an atomic concentration of 9.7%. This Ag validates the successful formation of AgNPs and aligns with results from the FT-IR and XRD, which also affirmed the functional groups and crystalline nature of the nanoparticles (Akalin 2024; Khan *et al*. 2025). The chemical composition profile also shows a considerable amount of oxygen (59.0% atomic, 38% weight) and carbon (18.2% atomic, 8.8% weight), that could be attributed to the presence of organic compounds from the leaf extract which acted as capping and stabilizing agents. These organic residues include flavonoids, polyphenols, proteins, and terpenoids that not only caused the reduction of Ag ions but also prevent the nanoparticles from agglomeration by forming a thin organic layer around them (He *et al.* 2017; Abbas *et al*. 2024). The presence of minor elements such as nitrogen (8.50%), phosphorus (0.73%), and sulphur (0.43%) were also detected signifying that the nanoparticles originate from amino acids, proteins, or phospholipids which are often found in the leaf matrix, and this further corroborates that these biomolecules played a role in the reduction as well as in the stabilization processes during formation of the nanoparticle (Fahim *et al.* 2024; Ibrahim *et al.* 2024).

Table 2: Elemental Composition of L-AgNPs

Element Number	Element Symbol		Element Name	Atomic concentration	Weight Concentration
47	Ag		Silver	9.71	42.14
8	O		Oxygen	59.05	38
6	C		Carbon	18.22	8.80

17	Cl		Chlorine	3.37	4.81
7	N		Nitrogen	8.50	4.79
15	P		Phosphorous	0.73	0.91
16	S		Sulphur	0.43	0.55
19	K		Potassium	0.00	0.00
20	Ca		Calcium	0.00	0.00

The image of the synthesized L-AgNPs, as revealed by Transmission Electron Microscopy (TEM) analysis (Fig. 11), further provides evidence of the formation, size distribution, and morphology of the AgNPs.

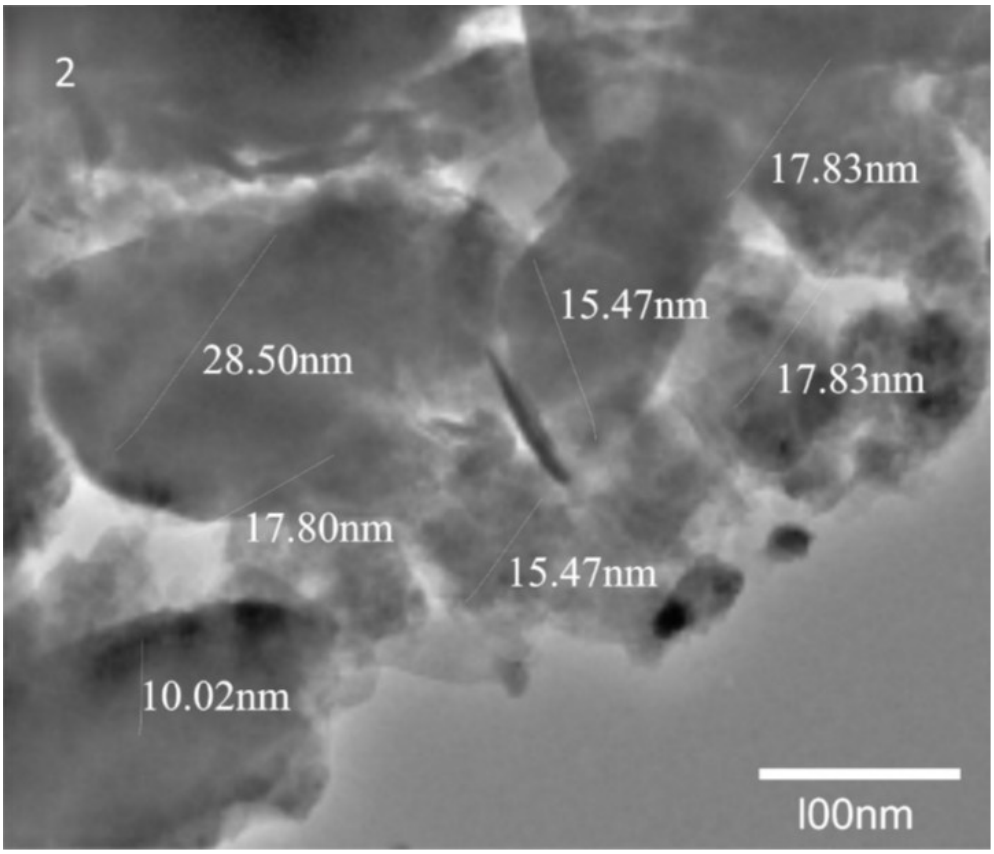

Fig. 11. TEM analysis of L-AgNPs

As depicted in the image (Fig. 11), the observed particles exhibited spherical to quasi-spherical morphology with particle size distribution in the range of 10.0 nm to 28.5 nm, affirming the nanoscale nature of the synthesized materials (He *et al.* 2017; Ibrahim *et al.* 2024). The presence of biomolecules in the leaf extract, which act as both reducing and capping agents, influence and cause variation in the particle size. These biomolecules control the growth and nucleation of AgNPs, averting excessive agglomeration and providing stability *via* surface functionalization. The presence of the biomolecules in the leaf extract effectively limited particle growth during synthesis, as evidenced by the small particle size observed, resulting in nanoparticles with good dispersion and stability. Related observations were made by Akalin (2024), where TEM analysis of green synthesized AgNPs using *Calluna vulgaris* leaf extract gave spherical shapes with sizes ranging from 12 to 25 nm, while Khan *et al*. (2025) reported particle size distributions in the range of 10 to 30 nm for AgNPs synthesized from *Withania coagulans* leaf extract.

Optical Sensing Ability with Selected Metals

Figure 12a indicates different metal ion solutions (Fe, As, Pb, Cd, and Mn), each exhibiting distinct colors or clarity depending on their ionic characteristics, while Fig. 12b represents the prepared synthesized L-AgNPs. Figure 12c depicts the appearance of L-AgNPs immediately after the addition of metal ion solutions (0 h), but after five days of incubation (d), distinct color variations were seen in all metal ion mixtures, suggesting surface modification or aggregation of the nanoparticle arising from metal ion binding.

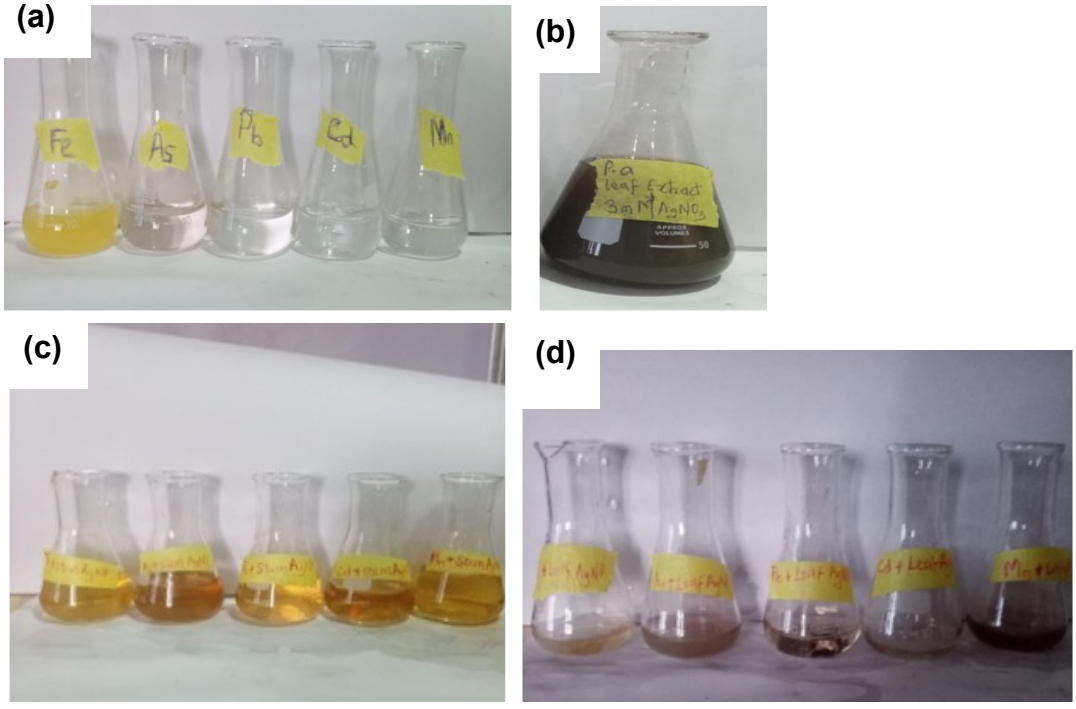

Fig. 12. (a) Different metal solution (b) L-AgNPs (c) after addition of metal solution to L-AgNPs at 0 hour, and (d) Color change after 5 days

These color changes provide qualitative evidence of the sensitivity of the synthesized nanoparticles toward specific heavy metals and demonstrate its potential application as colorimetric probes for environmental sensing applications. Figure 13

depicts the spectral from UV–Visible absorption of L-AgNPs and their response to various metal ions with noticeable spectral changes recorded. It was noticed that the prepared AgNPs demonstrated a strong and broad SPR band found in the range of 350 to 450 nm after interacting with the metal ions (Arif *et al*. 2024; Duman *et al*. 2024). The presence of Pb and Fe ions provided a great decrease in absorbance intensity with a blue shift of the SPR peak from 430 nm to 400 nm and 450 nm, respectively (Ibrahim *et al.* 2024). The ions of Cd and As caused moderate alterations with blue shift of the SPR peak from 450 to 350 nm, while Mn ions showed a distinct blue shift of the SPR peak enhancement around 430 to 450 nm, indicating strong interaction or possible reduction on the AgNP surface. These variations in wavelength position as well as in absorbance intensity reflect the differential interaction mechanisms and binding affinities of each metal ion with the AgNPs prepared (Arif *et al*. 2024; Duman *et al*. 2024). The results clearly demonstrate the sensitivity of the nanoparticles (L-AgNPs) to their surrounding environment as evident from the optical properties shown, thus making them efficient colorimetric sensors for metal detection. The combined observable color changes as well as spectral shifts provides a simple, rapid, and eco-friendly technique for monitoring metal ions in aqueous media.

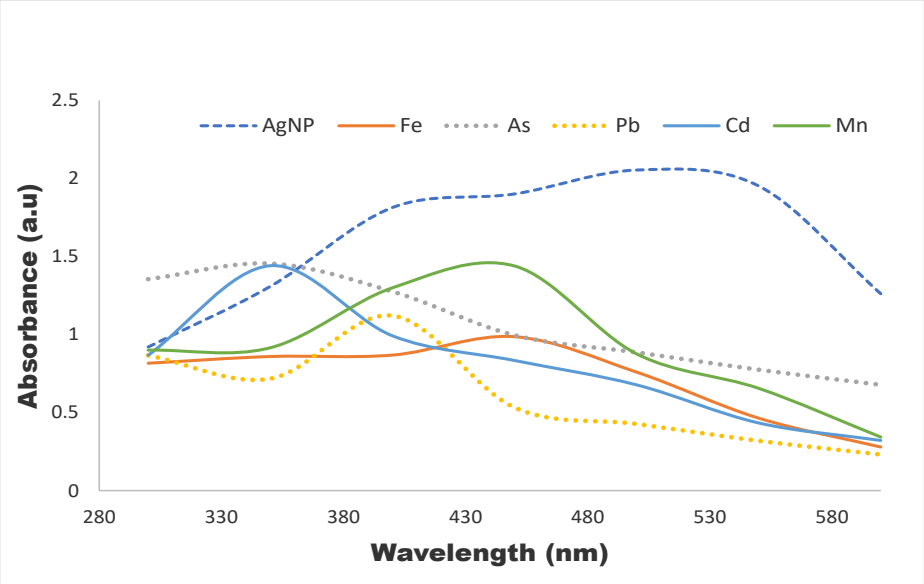

Fig. 13. Spectra of metal solutions with L-AgNPs

For metal-ion sensing, Babatimehin *et al*. (2025a) observed that green synthesized AgNPs showed distinct optical responses, including visible color changes and variations in absorbance intensity, upon the addition of the heavy metal ions Cu^{2+}, Pb^{2+}, and Cd^{2+}, with selective detection observed and that Pb^{2+} produced the most pronounced absorbance change. They attributed the shifts in wavelengths in the SPR band and reduced absorbance intensity to interactions between the nanoparticle surface and metal ions that likely involved aggregation or binding processes that modify the local dielectric environment of the AgNPs. A similar study conducted by Ibrahim *et al*. (2024) on the green synthesis of AgNPs found out that heavy-metal ion detection with UV–Vis caused a shift in Pb^{2+} SPR from 438 to 429 nm. In addition, Tamilselvan *et al*. (2022) observed that the presence of some heavy metal ions in aqueous media on interacting with AgNPs

produced the appearance of new absorbance peaks which was seen in the range of approximately 640 to 930 nm, in addition to the characteristic peak around 410 nm initially seen for the AgNPs. They stressed further, the addition of Pb^{2+} and Ni^{2+} ions caused a noticeable red shift of the SPR band from 410 nm to approximately 460 nm.

Antimicrobial Activities of L-AgNPs

The results obtained from the zone of inhibition (ZOI) assay are as shown in Fig. 14 and listed in Table 3, and the L–AgNPs synthesized demonstrated large inhibition zones of 28 mm for *S. aureus* and 38 mm for *E. coli*, which are higher than those of gentamicin (18 mm and 20 mm, respectively).

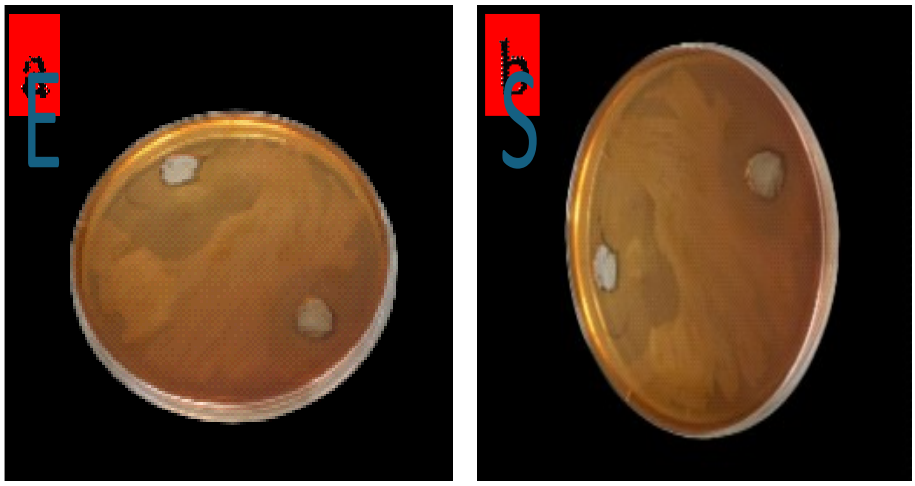

Fig. 14. Antibiotic sensitivity of (E1) L-AgNPs on *Escherichia coli, and* (S1) L-AgNPs on *Staphylococcus aureus.*

The high inhibitory activity of AgNPs produced reflects their strong bactericidal effect against both Gram-positive (*S. aureus*) and Gram-negative (*E. coli*) strains. The higher susceptibility of *E. coli* compared *S. aureus* could be because of differences in cell wall structure, as *E. coli* contains a thinner peptidoglycan layer and an outer membrane that permits easier penetration of nanoparticles, whereas *S. aureus* has a thicker cell wall that offers partial resistance (Akalin 2024; Khan *et al*. 2025). The greater performance of L–AgNPs compared to gentamicin could be as a result of the synergistic effects of the nanoparticles and the bioactive capping agents and small size (10 to 30 nm) derived from the leaf extract, which enables quick interaction with bacterial membranes and facilitate the generation of reactive oxygen species (Fahim *et al.* 2024). The results obtained for the MIC is listed in Table 4, which further corroborates the potent antibacterial ability of the fabricated AgNPs. The nanoparticles inhibited the growth of *E. coli* and *S. aureus* growth at very low concentrations of 2 and 4 µg/mL, respectively, as compared with gentamicin which required a higher concentration of 8 µg/mL for both bacteria to achieve similar inhibition. This implies that the biosynthesized AgNPs demonstrated higher sensitivity towards the test organisms (Khan *et al*. 2025). The result from this study is comparable to MIC values of 1 to 5 µg/mL, as reported by Akalin (2024) for green-synthesized AgNPs from *Withania coagulans* and *Calluna vulgaris* leaves. The MBC results, as shown in Table 5, reflects that L–AgNPs demonstrated bactericidal effects at very low concentrations of 2 µg/mL for both *S. aureus* and *E. coli,* whereas gentamicin needed 6

µg/mL to attain complete bacterial elimination. This indicates that the synthesized nanoparticles were more efficient in killing bacterial cells than the conventional antibiotic. The low values of MBC obtained from this work are consistent with previous reports, where AgNPs biosynthesized possess excellent bactericidal potential because of their multiple modes of action (Abbas *et al*. 2024; Fahim *et al*. 2024).

Table 3. Zone of Inhibition

AgNP	Inhibitory Zone (mm)	Inhibitory Zone (mm)
	E. Coli	*S. aureus*
Leaf (3 mM)	38	28
Gentamicin	18	20

Table 4. Minimum Inhibitory Concentration

AgNP	*E. coli*	*S. aureus*
Leaf (3 mM)	2 µg/mL	4 µg/mL
Gentamicin	8 µg/mL	8 µg/mL

Table 5. Minimum Bactericidal Concentration

AgNP	*E. coli*	*S. aureus*
Leaf (3 mM)	2 µg/ mL	2 µg/ mL
Gentamicin	6 µg/ mL	6 µg/ mL

Comparison of Key Physicochemical Characteristics and Applications of Green Synthesis of AgNPs

As illustrated in Table 6, the key physicochemical characteristics and applications of silver nanoparticles synthesized using different plant extracts reported in the literature were compared with those obtained in the present study. The comparison displays the similarities in SPR range (400 to 450 nm), predominantly spherical morphology, and nanoscale particle size distribution, while emphasizing the dual antibacterial and sensing functionality demonstrated in this work.

Table 6. Comparison of the Present Study with Selected Plant-Mediated Green Synthesis of AgNPs

Plant Source	Synthesis Conditions	SPR Peak (nm)	Particle Size (nm)	Morph-ology	Main Application (s)	Reference
Azadirachta indica (leaf)	Mild heating; aqueous extract	~420 to 440	10 to 30	Spherical	Heavy metal sensing	Babatimehin *et al*. 2025a
Phyllanthus amarus (leaf)	Ambient conditions; aqueous extract	~420 to 440	15 to 35	Spherical	Antimicrobial; catalytic	Ajitha *et al*. 2018
Aloe succotrina (leaf)	Controlled temperature; aqueous extract	~410 to 430	15 to 50	Spherical	Antibacterial; drug delivery potential	Fahimmunisha *et al*. 2020
Psidium guajava (leaf)	Mild heating; aqueous extract	~420 to 450	20 to 45	Mostly spherical	Toxicity evaluation; antimicrobial	Albadawi *et al*. 2024
Vachellia tortilis (leaf)	pH 10; 70 °C	~438	15 to 40	Spherical	Heavy metal sensing	Ibrahim *et al*. 2024
Alpinia katsumadai (seed)	Room temperature; aqueous extract	~420	10 to 35	Spherical	Antioxidant; antibacterial	He *et al.* 2017
Withania coagulans (leaf)	Alkaline pH; moderate heating	~430 to 445	10 to 30	Spherical	Antioxidant; antimicrobial	Khan *et al.* 2025
Calluna vulgaris (leaf)	Mild heating; neutral to basic pH	~430	12 to 25	Spherical	Antibacterial; photocatalytic	Akalin 2024
Phyllanthus amarus (leaf)	1 to 3 mM $AgNO_3$; optimized pH 8 to 9; 60 to 70 °C	400 to 450	10.02 to 28.5	Spherical/ quasi-spherical	Heavy metal sensing; antibacterial	**Present study**

CONCLUSIONS

From this study on the use of *Phyllanthus amarus* leaf extract for the synthesis of silver nanoparticles, the following can be deduced:

1. *Phyllanthus amarus* extract effectively mediated the eco-friendly production of silver nanoparticles (AgNPs).
2. The presence of bioactive compounds responsible for nanoparticle stabilization and reduction was confirmed from gas chromatography-mass spectrometry (GC-MS) analysis.
3. Structural examinations with X-ray diffraction (XRD), Fourier transform infrared (FTIR), transmission electron microscopy (TEM), and energy-dispersive X-ray (EDX) analyses validated the crystalline, spherical, and phytochemical-capped nature of the prepared AgNPs.

4. The as-prepared nanoparticles demonstrated strong optical responses toward metal ions highlight their promise as rapid, green colorimetric sensors for monitoring the environment.
5. The biosynthesized AgNPs showed superior antibacterial efficacy compared to gentamicin.
6. For future work**, t**he dual functional properties exhibited in this study signify that these biogenic AgNPs could be further explored for integration into portable sensing devices for on-site heavy metal detection and in antimicrobial coatings or wound-care formulations. Future study may focus on large-scale synthesis optimization, toxicity evaluation, long-term stability assessment, and real-sample environmental validation to advance their practical deployment.

ACKNOWLEDGMENTS

Princess Nourah bint Abdulrahman University Researchers Supporting Project number (PNURSP2026R76), Princess Nourah bint Abdulrahman University, Riyadh, Saudi Arabia. The authors extend their appreciation to the Deanship of Scientific Research at Northern Border University, Arar, KSA, for funding this research work through the project number "NBU-FFR-2026-2985-04"

Authors Contributions

Ghaferah H. Al-Hazmi and Ali El-Rayyes: Contributed Resources, Software, Funding acquisition; Lamia A. Albedair: Project administration, Contributed Resources, Writing – Review & Editing; Edwin Andrew Ofudje: Conceptualization, Investigation, and supervised the work; Moamen S. Refat: Visualization, Validation, Writing – Review & Editing; Kholoud K. Alzahrani: Formal analysis, Software, Writing – Review & Editing; Oyebola Elizabeth Ogunbamowo and Abidemi Mercy Babatimehin: Methodology, Data curation, Writing – Original Draft

REFERENCES CITED

Abbas, R., Luo, J., Qi, X., Naz, A., Khan, I. A., Liu, H., Yu, S., and Wei, J. (2024). "Silver nanoparticles: synthesis, structure, properties and applications," *Nanomaterials* 14(17), article 1425. https://doi.org/10.3390/nano14171425

Abdelmonem, B. H., Kamal, L. T., Elbaz, R. M., Khalifa, M. R., and Abdelnaser, A. (2025). "From contamination to detection: The growing threat of heavy metals," *Heliyon* 5, 11(1), article e41713. https://doi.org/10.1016/j.heliyon.2025.e41713

Ahmed, T., Ogulata, R. T., and Gülnaz, O. (2024). "Multifarious uses of UV-VIS spectroscopy for green synthesis of silver nanoparticles for antibacterial textiles," *Textile and Leather Review* 7, 176-202. https://doi.org/10.31881/TLR.2024.014

Ajitha, B., Reddy, Y. A. K., Jeon, H. J., and Ahn, C. W. (2018). "Synthesis of silver nanoparticles in an eco-friendly way using *Phyllanthus amarus* leaf extract: Antimicrobial and catalytic activity," *Advanced Powder Technology* 29(1), 86-93. https://doi.org/10.1016/j.apt.2017.10.015

Akalin, G. O. (2024). "Green synthesis of silver nanoparticles using leaf extract of *Calluna vulgaris*: Characterizations, properties, and photocatalytic activities," *BioResources* 19(3), 4396-4422. https://doi.org/10.15376/biores.19.3.4396-4422

Akinhanmi, T. F., Ofudje, E. A., Adeogun, A. I., Aina, P., and Joseph, I. M. (2020). "Orange peel as low-cost adsorbent in the elimination of Cd (II) ion: Kinetics, isotherm, thermodynamic and optimization evaluations," *Bioresources and Bioprocessing* 7(1), article 34. https://doi.org/10.1186/s40643-020-00320-y

Albadawi, E. A., Musa, E. N. A., Ghaban, H. M., Ebrahim, N. A., Albadrani, M. S., and El-Tokhy, A. I. (2024). "Eco-friendly green synthesis of silver nanoparticles from guajava leaves extract for controlling organophosphorus pesticides hazards, characterization, and in-vivo toxicity assessment," *BMC Pharmacol. Toxicol.* 25, article 98. https://doi.org/10.1186/s40360-024-00826-7

Anandalakshmi, K., Venugobal, J., and Ramasamy, V. (2016). "Characterization of silver nanoparticles by green synthesis method using *Pedalium murex* leaf extract and their antibacterial activity," *Appl. Nanosci.* 6, 399-408. https://doi.org/10.1007/s13204-015-0449-z

Arif, M., Raza, H., and Akhter, T. (2024). "UV-Vis spectroscopy in the characterization and applications of smart microgels and metal nanoparticle-decorated smart microgels: A critical review," *RSC Adv.* 14, 38120-38134. https://doi.org/10.1039/D4RA07643E

Babatimehin, A. M., Ajayi, G. O., Ogunbamowo, O. E., El-Rayyes, A., Albedair, L. A., Alsuhaibani, A. M., and Ofudje, E. A. (2025a). "Synthesis of silver nanoparticles using Azadirachta indica leaf extracts for heavy metal sensing," *BioResources* 20(2), 3342-3366. https://doi.org/10.15376/biores.20.2.3342-3366

Babatimehin, A. M., Ogunbamowo, O. E., Ajayi, G. O., Gamal, A. E., Emran, T. B., Ofudje, E. A., and Hefnawy, M. (2025b). "Colorimetric sensing of chlorpyrifos pesticides using green synthesized silver nanoparticles from neem root extracts," *BioResources* 20(3), 6948-6965. https://doi.org/10.15376/biores.20.3.6948-6965

Bruna, T., Maldonado-Bravo, F., Jara, P., and Caro, N. (2021). "Silver nanoparticles and their antibacterial applications," *International Journal of Molecular Sciences* 22(13), article 7202. https://doi.org/10.3390/ijms22137202

Chen, W., Liu, Q., Tian, S., and Zhao, X. (2019). "Exposed facet dependent stability of ZnO micro/nano crystals as a photocatalyst," *Applied Surface Science* 470, 807-816. https://doi.org/10.1016/j.apsusc.2018.11.206

Dhir, R., Chauhan, S., Subham, P., Kumar, S., Sharma, P., Shidiki, A., and Kumar, G. (2024). "Plant-mediated synthesis of silver nanoparticles: unlocking their pharmacological potential–a comprehensive review," *Frontiers in Bioengineering and Biotechnology* 11, article 1324805. https://doi.org/10.3389/fbioe.2023.1324805

Duman, H., Eker, F., Akdaşçi, E., Witkowska, A. M., Bechelany, M., and Karav, S. (2024). "Silver nanoparticles: A comprehensive review of synthesis methods and chemical and physical properties," *Nanomaterials* 14(18), article 1527. https://doi.org/10.3390/nano14181527

Fahimmunisha, B. A., Ishwarya, R., AlSalhi, M. S., Devanesan, S., Govindarajan, M., and Vaseeharan, B. (2020). "Green fabrication, characterization and antibacterial potential of zinc oxide nanoparticles using *Aloe socotrina* leaf extract: A novel drug delivery approach," *Journal of Drug Delivery Science and Technology* 55, article 101465. https://doi.org/10.1016/j.jddst.2019.101465

Fahim, M., Shahzaib, A., Nishat, N., Jahan, A., Bhat, T.A. and Inam, A. (2024). "Green synthesis of silver nanoparticles: A comprehensive review of methods, influencing factors, and applications," *JCIS Open* 16, article 100125. https://doi.org/10.1016/j.jciso.2024.100125

Habeeb Rahuman, H. B., Dhandapani, R., Narayanan, S., Palanivel, V., Paramasivam, R., Subbarayalu, R., Thangavelu, S., and Muthupandian, S. (2022). "Medicinal plants mediated the green synthesis of silver nanoparticles and their biomedical applications," *IET Nanobiotechnology* 16(4), 115-144. https://doi.org/10.1049/nbt2.12078

Khan, A., Younis, T., Anas, M. , Ali, M., Shinwari, Z. K., Khalil, A. T., Munawar, K. S., Mohamed, H. E. A., Hkiri, K., Maaza, M., Seleiman, M.F., and Khan, N. (2025). "*Withania coagulans*-mediated green synthesis of silver nanoparticles: Characterization and assessment of their phytochemical, antioxidant, toxicity, and antimicrobial activities," *BMC Plant Biol* 25, article 574. https://doi.org/10.1186/s12870-025-06533-7

Khorrami, S., Zarepour , A., and Zarrabi, A. (2019). "Green synthesis of silver nanoparticles at low temperature in a fast pace with unique DPPH radical scavenging and selective cytotoxicity against MCF-7 and BT-20 tumor cell lines," *Biotechnology Reports* 24, article e00393. https://doi.org/10.1016/j.btre.2019.e00393

Kyabutwa, P. L., Alyamni, N., Abot, J. L., and Zestos, A. G. (2025). "Recent trends in electrochemical methods for real-time detection of heavy metals in water and soil: A review," *Curr. Opin. Electrochem*. 54, article 101749. https://doi.org/10.1016/j.coelec.2025.101749

He, Y., Wei, F., Ma, Z., Zhang, H., Yang, Q., Yao, B., Huang, Z., Li, J., Zeng, C., and Zhang, Q. (2017). "Green synthesis of silver nanoparticles using seed extract of *Alpinia katsumadai*, and their antioxidant, cytotoxicity, and antibacterial activities," *RSC Advances* 7(63), 39842-39851. https://doi.org/10.1039/C7RA05286C

Helim, R., Zazoua, A., and Korri-Youssoufi, H. (2024). "Sustainable biopolymer-based electrochemical sensors for trace heavy metal determination in water: A comprehensive review," *Chemosensors* 12(12), article 267. https://doi.org/10.3390/chemosensors12120267

Ibrahim, N. H., Taha, G. M., Hagaggi, N. S. A., and Moghazy, M. A. (2024). "Green synthesis of silver nanoparticles and its environmental sensor ability to some heavy metals," *BMC Chemistry* 18, article 7. https://doi.org/10.1186/s13065-023-01105-y

Joseph, J., Keren, D. S., Raghavi, R., Mary, S. A., and Aruni, W. (2021). "Green synthesis of silver nanoparticles using *Phyllanthus amarus* seeds and their antibacterial activity assessment," *Biomedical and Biotechnology Research Journal* 5(1), 35-38. https://doi.org/10.4103/bbrj.bbrj_139_20

Jomova, K., Alomar, S. Y., Nepovimova, E., Kuca, K., and Valko, M. (2025). "Heavy metals: Toxicity and human health effects," *Arch Toxicol* 99, 153-209. https://doi.org/10.1007/s00204-024-03903-2

Khalir, W. K. A. W. M., Shameli, K., Jazayeri, S. D., Othman, N. A., Che Jusoh, N. W., and Hassan, N. M. (2020). "Biosynthesized silver nanoparticles by aqueous stem extract of *Entada spiralis* and screening of their biomedical activity," *Front Chem.* 8, article 620. https://doi.org/10.3389/fchem.2020.00620

Lokhande, R. S., Singare, P. U., and Pimple, D. S. (2011). "Toxicity study of heavy metals pollutants in wastewater effluent samples collected from Taloja industrial

estate of Mumbai, India," *Resources and Environment* 1(1), 13-19. https://doi.org/10.5923/j.re.20110101.02

Maimaiti, X., Bassey, A. P., Liu, X., Zhu, Y., Fan, L., Rahman, N., Luo, R., Wang, F., and Wang, Y. (2024). "Green synthesis of silver nanoparticles using *Houttuynia cordata* Thunb rhizome extracts and their antibacterial potential against common foodborne pathogens," *Int. J. Food Sc. and Technol.* 59(5), 283-3296. https://doi.org/10.1111/ijfs.17074

Md Monir, H., Hamza, A., Polash, S. A., Tushar, M. H., Takikawa, M., Piash, A. B., Dekiwadia, C., Saha, T., Takeoka, S., and Sarke, S. R. (2024). "Green synthesis of silver nanoparticles using *Phyllanthus emblica* extract: Investigation of antibacterial activity and biocompatibility *in vivo*," *RSC Pharm* 1, 245-258. https://doi.org/10.1039/D3PM0077J

Moideen, R. S., and Prabha, A. L. (2022). "Plant mediated synthesis of silver nanoparticles from leaf extract of *Phyllanthus amarus L*. and their antibacterial activity," *International Journal of Botany Studies* 7(1), 251-257

Njideaka, O. T., Onyeukwu, O. B., and Dibie, D. C. (2024). "Antioxidant and phytochemical analysis of methanol extract of *phyllanthus amarus*," *FUDMA Journal of Sciences* 8(5), 295-299. https://doi.org/10.33003/fjs-2024-0805-2724

Nkosi, N. C., Basson, A. K., Ntombela, Z. G., Dlamini, N. G., and Pullabhotla, R. V. S. R. (2024). "Green synthesis, characterization and application of silver nanoparticles using bioflocculant: A review," *Bioengineering* 11(5), article 492. https://doi.org/10.3390/bioengineering11050492

Ofudje, E. A., Adedapo, A. E., Oladeji, O. B., Sodiya, E. F., Ibadin, F. H., and Zhang, D. (2021). "Nano-rod hydroxyapatite for the uptake of nickel ions: Effect of sintering behaviour on adsorption parameters," *Journal of Environmental Chemical Engineering* 9(5), article 105931. https://doi.org/10.1016/j.jece.2021.105931

Ogunbamowo, O. E., El-Rayyes, A., Hefnawy, M., El Gamal, A., Babatimehin, A. M., Maloma, M. R., Sodiya, E.F., and Ofudje, E. A. (2025). "Optical and phytochemical detection of decayed food items using yeast mediated silver nanoparticle," *Bulletin of the Chemical Society of Ethiopia* 39(5), 921-936. https://doi.org/10.4314/bcse.v39i5.9

Nadumane, S.S., Biswas, R., and Mazumder, N. (2024). "Integrated microfluidic platforms for heavy metal sensing: a comprehensive review," *Anal. Methods* 16, 2810-2823. https://doi.org/10.1039/D4AY00293H

Palanisamy, S., David, R., Madav, E., Kannan, V. D. Rajendran, V., Sampath, S., Ahmed, M. Z., Alqahtani, A. S., Kazmi, S., and Asaithambi, P. (2024). "Green fabrication of silver nanoparticles using leaf extract of tropical vine *Momordica charantia*: Spectral characterization and *in vitro* cytotoxicity evaluation on human breast cancer cells," article 2304428. https://doi.org/ 10.1080/10667857.2024.2304428

Paithankar, J. G., Saini, S., Dwivedi, S., Sharma, A., and Chowdhuri, D. K. (2021). "Heavy metal associated health hazards: An interplay of oxidative stress and signal transduction," *Chemosphere* 262, article 128350. https://doi.org/10.1016/j.chemosphere.2020.128350

Tamilselvan, S., Soniya, R. M., Vasantharaja, R., Kannan, M., Supriya, S., Batvari, B. P. D, Ramesh, T., and Govindaraju, K. (2022). "Silver nanoparticles based spectroscopic sensing of eight metal ions in aqueous solutions," *Environmental Research* 212(Part E), article 13585. https://doi.org/10.1016/j.envres.2022.113585

Velgosova, O., Mačák, L., Lisnichuk, M., and Varga, P. (2025). "Influence of pH and temperature on the synthesis and stability of biologically synthesized AgNPs," *Applied Nano*. 6(4), article 22. https://doi.org/10.3390/applnano6040022

World Health Organization (WHO). (2013). "Ten chemicals of major public health Concern," *World Health Organization* 14

Zeheri, A. H., Taher, M., Mohd Jailani, M. T., Md Jaffri, J., Darnis, D. S., and Khotib, J. (2025). "Green synthesis of silver nanoparticles using *Aidia densiflora* leaf extract: Characterization and bioactivities," *Journal of Pharmacy* 5(2), 256-270. https://doi.org/10.31436/jop.v5i2.390

Article submitted: December 4, 2025; Peer review completed: February 15, 2026; Revised version received and accepted: February 15, 2026; Published: February 26, 2026.
DOI: 10.15376/biores.21.2.3518-3542